Numerical Modeling of Soil-Pile-Interaction with Near and Far Field Earthquake's Effects

M. Shahmohammadi Mehrjardi [a*], A.A. Fallah [b], S.T. Tabatabaei Aghda [c]

[a] *M.Sc. Graduate, Civil and Earthquake Engineering, Islamic Azad University, Maybod, Iran.*

[b] *Assistant Professor, Islamic Azad University of Maybod, Maybod, Iran.*

[c] *Faculty Member, BHRC (Road, Housing & Urban Development Research Center), Tehran, Iran.*

Abstract

This paper studies Near and Far Field effects of the response of a column-pile to earthquakes considering Dynamic-Soil-Structure-Interaction (DSSI) effects in soft clay (Vs<180 m/s) and stiff clay (180<Vs<375 m/s). Opensees software that can simulate the dynamic time history analysis is used. Both kinematic and inertial interactions are considered and Finite Element Method (FEM) is used to solve DSSI. The direct method applies to 3D modeling of the layered soil and column-pile. A Pressure Independ Multi Yield Surface Plasticity Model is used to simulate different kinds of clay behavior. Time history seismic analyses provide for the mass and stiffness matrices to evaluate dynamic structural response with and without directivity effects for Near and Far Field earthquakes. Results show that the Multi-Yield-Surface-Kinematic-Plasticity-Model can be used instead of bilinear springs between piles and clay soil, for both Near Field and Far Field earthquakes. In addition, comparing Near and Far Field analyses, acceleration response spectrum at the top of the structure in the Far Field increases with the softness of the soil more than that in the Near field.

Keywords: Dynamic Soil-Structure-Interaction; Multi Surface (Von Mises) Plasticity Model; Opensees; Near Field and Far Field Earthquake; Soft and Stiff clay.

1. Introduction

To understand the behavior of pile-column in a nonlinear modeling of soil considering soil-pile-structure-interaction, considering Near and Far Field is designated for earthquakes. Based on the previous studies, Near Field ground motions can make ground motion features naturally different from those in the Far Field due to forward rupture directivity, fling step effects, vertical seismic component, velocity pulse, hanging wall and footwall and vertical earthquake ground motion [1, 2]. The effect of forward directivity pulse (forward directivity pulse happens when the front rupture spreads toward the site, and the fault slip direction is aligned with the site [3]) and fling step play a crucial role in the Near Field earthquake because of the large energy that can cause considerable structural damage during an earthquake. Figure 1 shows that the velocity and displacement of near fault ground motion and displacements follow directions that are dominated by the fault geometry such as strike and fault rupture propagation.

Winkler foundation, Finite Element, and Boundary Element methods have been used in the soil-structure-pile-interaction analysis. Paying attention to the elastic modulus of the structure, interface of the pile-soil systems and structure material is significant for resonant amplitude and natural frequency [4].

We should consider that the plastic hinge in the pile is not allowed by code rules and specifications owing [5] to three main reasons: (i) plastic hinge locations are not accessible to repair after the strong ground motions which can

---

cause nonlinear behavior of structures, (ii) the high cost of repair of a badly damaged pile, (iii) capacity of unwanted destruction piles before entering superstructure is different from complete structure. However, plastic hinge in the pile cannot be avoided in strong earthquakes [6].
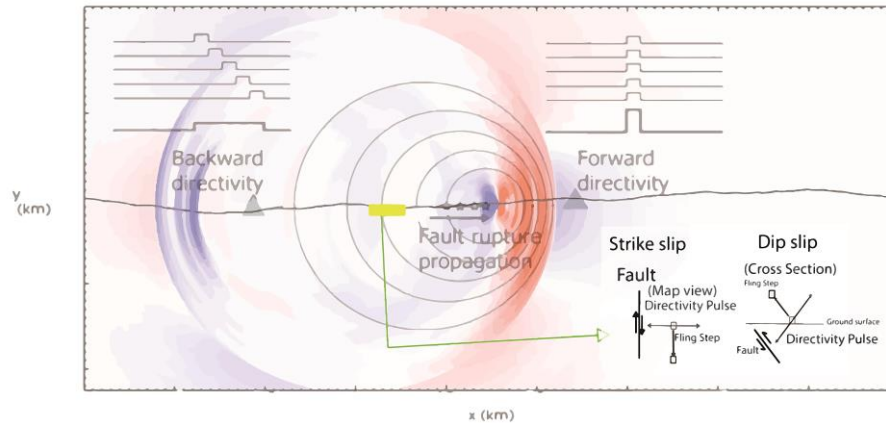
Figure 1. Forward and backward directivity effects [1, 7]**, and schema of the rupture directivity pulse between the strike-normal fault and strike-parallel fault components of ground displacement** [8]

In order to remove the reflecting waves, the velocity of plain wave approximation node is calculated by [9]:

$$p = \rho c \tag{1}$$

Where p is pressure vector, ρ is the media density and c is velocity of sound. Nevertheless, Equation 1. does not consider mass effects.

According to the absorbing boundary condition of Lysmer and Kuhlemeyer [10], the most effective expression is indicated by σ=aρVpŭ for primary waves and τ=bρVsŭ for secondary waves. In these equations, ρ is the media density (such as soil density), ŭ represents the velocities in 3 directions (x,y,z), a & b are dimensionless parameters that were suggested a=b=1.0 [10]. Vp (primary velocities) and Vs (secondary velocities) can be obtained by the following equations:

$$V_p = \sqrt{\frac{E(1-\nu)}{\rho(1-2\nu)(1+\nu)}} = \sqrt{\frac{2G(1-\nu)}{\rho(1-2\nu)}} \tag{2}$$

$$V_s = \sqrt{\frac{E}{2\rho(1+\nu)}} = \sqrt{\frac{G}{\rho}} \tag{3}$$

Where:

E: young's modulus (tensile elasticity)

ν: Poisson's ratio

G: Shear modulus

The equation of motion of the dynamic-soil-structure-system can be written as:

$$[M]\left\{\frac{\partial^2 u}{\partial t^2}\right\} + ([C] + [D])\left\{\frac{\partial u}{\partial t}\right\} + [K]\{u\} + [K_{nl}]\{u\} = -[M]\{m\}\frac{\partial^2 u_g}{\partial t^2} \tag{4}$$

Where $\{u\}$ is nodal displacements relative to the underlying soil and pile and $[K_{nl}]\{u\} = \{Fv\}$ is the force vector related to the viscous boundaries. This vector vanishes when there is no difference between Near Field motion of the artificial boundary and the free field motion [11]. [M] and [K] refer to the mass matrix and the stiffness matrix, respectively. D can be obtained the Raleigh damping matrix equation [12]:

$$[D] = a_0[M] + a_1[K] \tag{5}$$

In the numerical analysis, including plastic behavior of the structure, the stiffness (K_{nl}) and damping matrices should be the tangential matrices, which are updated at each time step t.

In the direct method of soil structure interaction using finite element programming, the element force can be obtained directly and does not need to be integrated from element nodes. This is correct for elastic beam or trust.

$$[R] = [K]\{u\} \tag{6}$$

Where R is resistment force vector and K is tangent modulus.

$$\frac{\partial R}{\partial t} = \frac{\partial k}{\partial t} \times u \tag{7}$$

According to the gauss quadrature, each element of the structure is evaluated by:

$$R_{(u_{n+1},t)} = \sum_{n=1}^{0} \int_{\Omega e} \phi_{(x)} . f_{(x)} . d\Omega_e \tag{8}$$

Which, in terms of nodal coordinates takes the following form:

$$R_{(u_{n+1},t)} = \sum_{1}^{m} w_m \phi_{(\varepsilon^m)} . f_{(\varepsilon^m)} . \left| J_{x,\varepsilon}^m \right| \tag{9}$$

Where W_m is weight factor, ε^m is the local coordinate at Gauss point m, $\phi_{(\varepsilon m)}$ is the first order difference between the shape function concerning coordinate and calculated at Gauss point m, and $\left| J_{x,\varepsilon}^m \right|$ is determinant of the Jacobian calculated at Gauss point m [13].

A Boundary Element (BEM) formulation using differential-algebraic equations (DAE) has been proposed in the literature [14]. The fundamental idea of this method is to formulate the equation of motion of the unbounded domain in the form of an integral equation instead of a differential equation by the Jacobian Matrix. The analysis procedure is illustrated using the flowchart in Kampitsis et al. [14].

1.1. Multi-Yield-Surface-Plasticity-Model

Multi yield surface J2 plasticity model is implemented in Opensees by Elgamal et al. [15]. The tangent stiffness matrix, which is based on the continuum tangent moduli, is used in Elgamal et al. study. The multi yield surface J2 plasticity model demonstrates the conception of plastic moduli to obtain a better description of the material plastic behavior under cyclic loadings, such as earthquakes in comparison with the Von Mises (the plasticity model with a single surface) [16] (Figure 2). That field is described by the accumulation of Nested yield surfaces by size constancy. Soil nonlinear shear behavior is displayed in Figure 2.
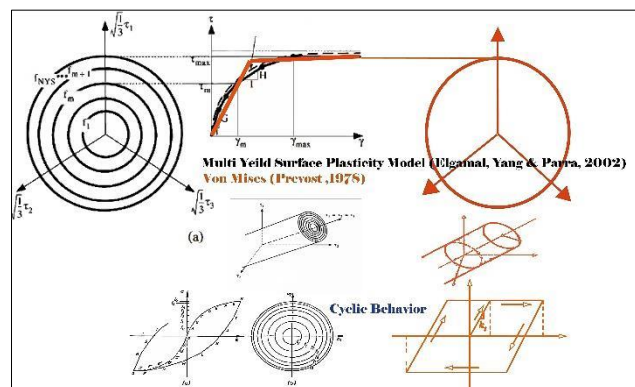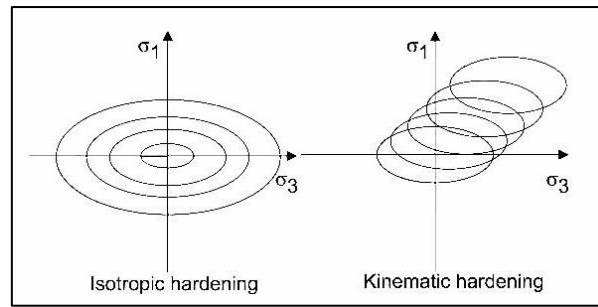

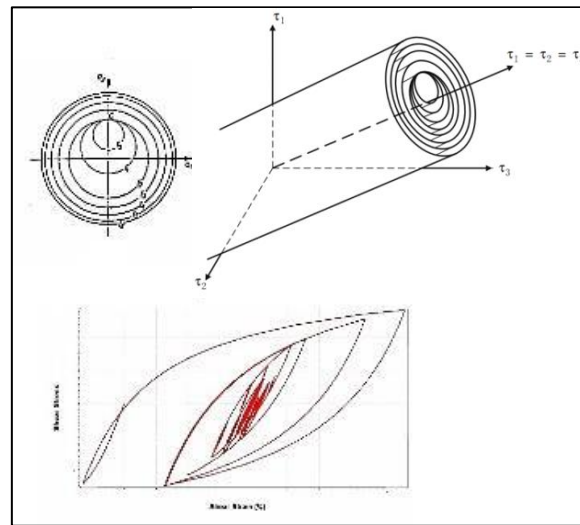**Figure 2. Multi-Yield-Surface-Plasticity-Model (Von Mises Shape) VS. Von Mises [15, 16]**

2. Hardening Rule

The nonlinear kinematic hardening rule explains change of the shape and size of the yield surface as plastic deformation occurs. Two types of hardening are demonstrated in Figure 3.

Figure 3. Schematic of two hardening types [17]

Elgamal et al. have developed kinematic hardening for clay soil and other materials in multi-yield-surface J2 plasticity [18, 19] which is shown in Figure 4.


Figure 4. Multi-yield-surface kinematic plasticity model [18, 19]

2.1. Verifying

In order to verify the accuracy and efficiency of a Soil-Pile-Structure-Interaction model analysis, the accuracy of the components of the model is verified by Kampitsis et al. study [14].

In Kampitsis et al. studies, the soil has nonlinear behavior and is linked to the pile with p-y springs connected to viscoelastic (Kelvin-Voigt) series as suggested by Wang et al. [20]. Soil springs are assigned along the length of the pile and correspond to forcing function. These springs can consider the Near Field plastification and the Far Field elastic character of the soil. Soil modeling based on spring and dashpot supported boundary conditions ignore radiation damping and kinematic effects [21] (the free field boundaries were investigated by 3 dashpots on each node on the boundaries and alternatively appropriate Multi-Point Constrains boundaries) [21]. The height of the column-pile is 40 m that is embedded in two layers of the clay. The column-pile diameter is 1.5 mترکیب; other characteristics are shown in Figure 5. Furthermore, a table of soils parameters is presented in Table 1.

To estimate the seismic motion at various depths below the ground surface, deconvolution analyses are required, which is done using Opensees. A layered soil profile is modeled in 2D using nodes with 2DOF (Figure 6). For this aim, the target 0.8 g acceleration time history is used as input. Then the motion at the depth of 30 m is extracted [14].
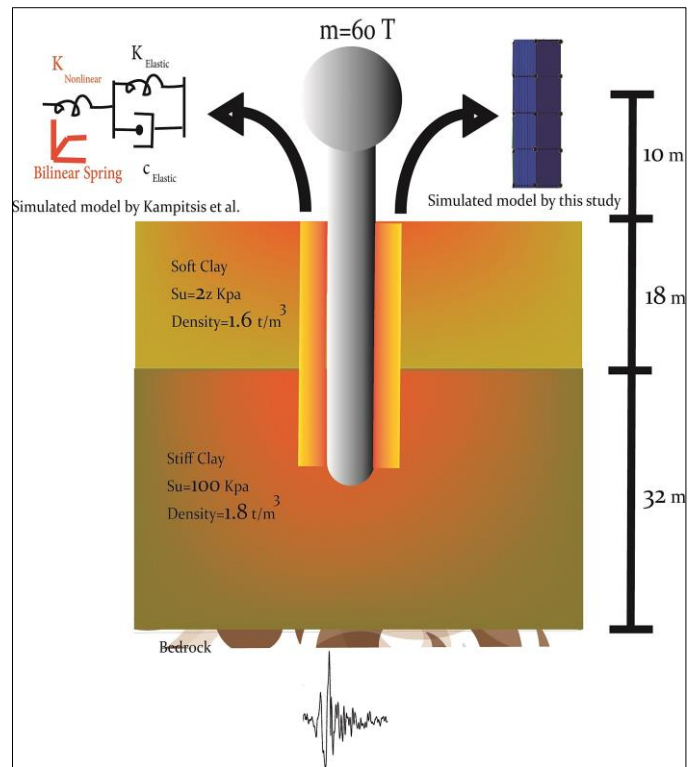
Figure 5. Simulated model by Kampitsis et al.

Table 1. Soil parameters of verification

Properties	Soft Clay	Stiff Clay
Mass Density (t/m3)	1.6	1.8
Shear modulus (KPa)	49730.7	200000
Bulk modulus (KPa)	107749.9	433333.3
Poisson's Ratio	0.3	0.3
Cohesion (KPa)	26	100
Permeability co. eff (m/s)	10-9	10-7
Friction angle (deg.)	0	0
Peak Shear Strain	0.03	0.03
Number of Yield Surfaces	20	20
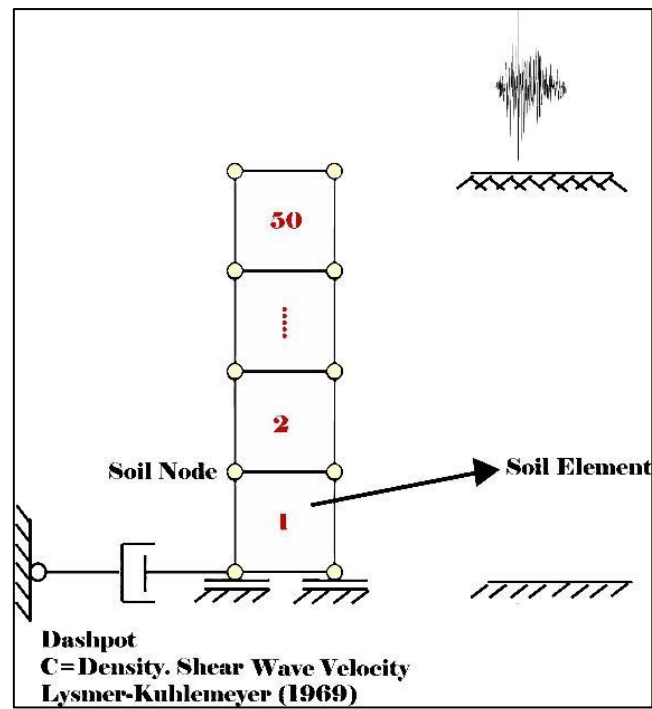
Figure 6. Deconvolutionan analysis in Opensees

The acceleration time history at the bedrock is presented in Figure 7, and Figure 8. is the validated model compared to the model proposed by Kampitsis et al.
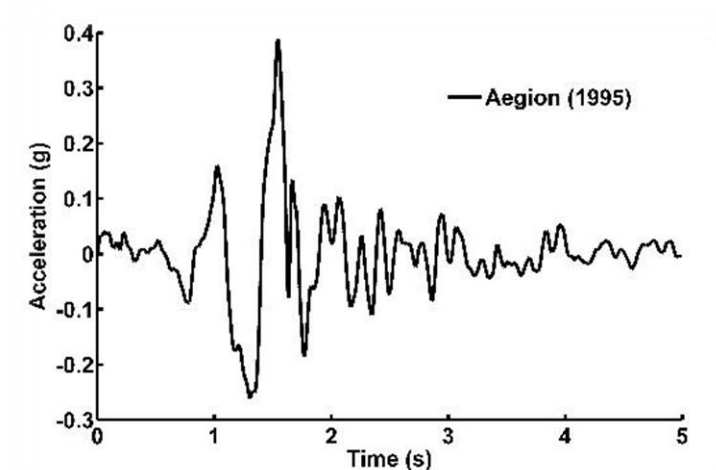

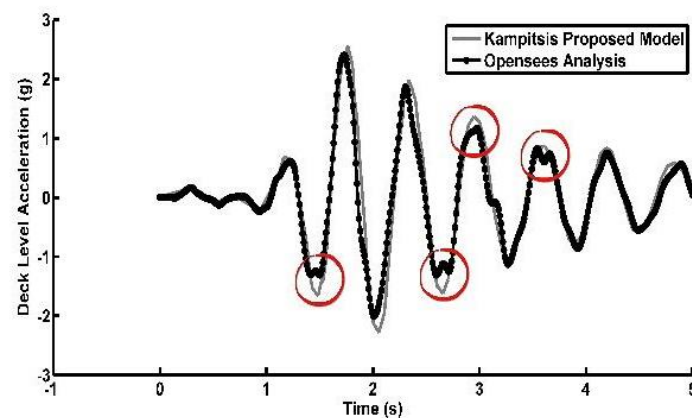**Figure 7. Ground motion time history used in the verification analysis**

Figure 8. Model verification of deck level acceleration

Red circles show different shapes between deck level acceleration response of bilinear springs and multi-yield-surface-plasticity material, which is used for the interface (Figure 8). Furthermore, displacement time history of numerically simulated response agrees well with the corresponding Kampitsis et al. study result (Figure 9). Moreover, maximum deck level displacement for this analysis is about 22 cm (Figure 10). Percentage error is computed for the deck level acceleration in order to assess the accuracy of validation. Percentage error is based on equation (10) for each point.

$$Error\ Percentage = \frac{(Value_{KPM} - Value_{OA})}{Value_{KPM}} * 100 \tag{10}$$

Matlab software is employed for writing the code. The Percentage Error contours of deck level acceleration are shown in Figure 11, which indicates that the maximum relative error through equation (10) is less than 3%.
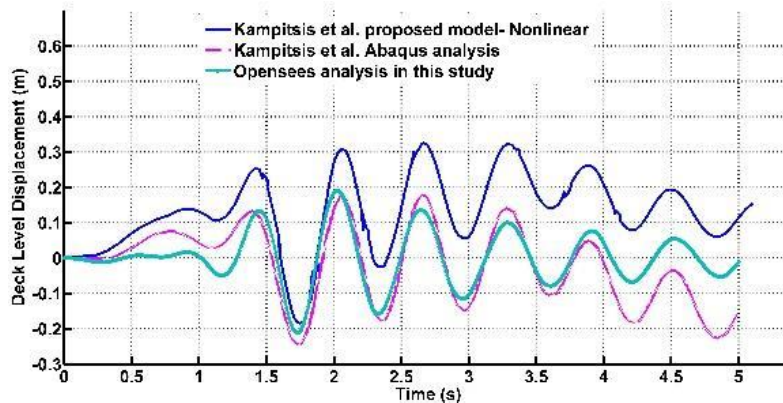
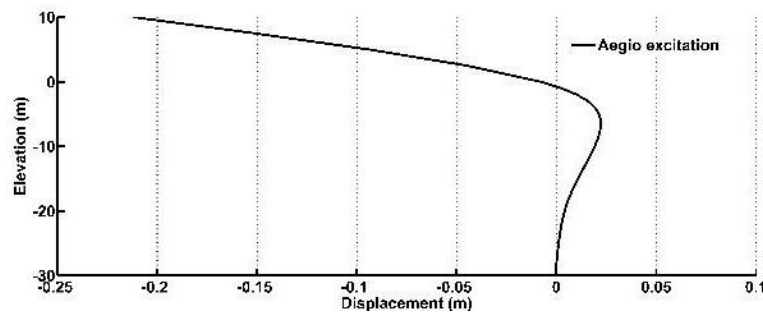**Figure 9. Model verification of deck level displacement**

Figure 10. The result of maximum horizontal displacement of column-pile (two)
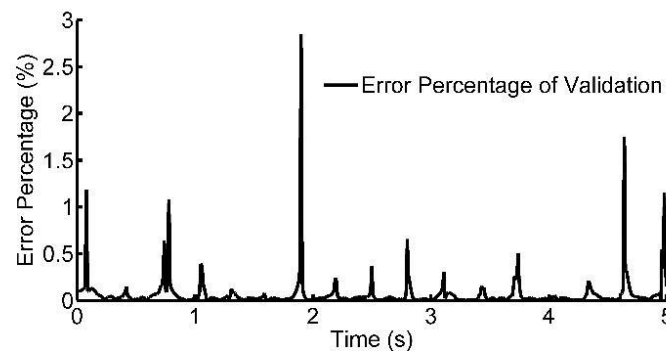
**Figure 11. Percentage of error**

2.2. Details of Model

Opensees has been used to create and analyze the three dimensional FE models of this study in dynamic time history [22]. The column-pile is idealized as beam structure with elastic behavior (Table 2). In this study, 3D soil domain and a Pressure In depending Multi Yield elastic-plastic constitutive model is used to model the soil behavior in models. The soil domain is discretized by 8 nodes solid element. For piles embedded in soft clay, significant yielding may occur at the pile-soil interface. Interface materials were used to model soil pile interaction, as shown in Figure 14. Each material of interface meshes differently. As it is shown, the plastic material uniformly meshes in 9 patterns. Other properties of meshing and the shape of the model are the same as Figure 12 and Figure 13.

Table 2. Column-Pile Specifications

Dimension and Properties of Circular Column-Pile	
Moment of Inertia (m^4)	0.2485
Mass Density (t/m^3)	4.417
Column Diameter (m)	1.5
Young's Modulus (GPa)	30
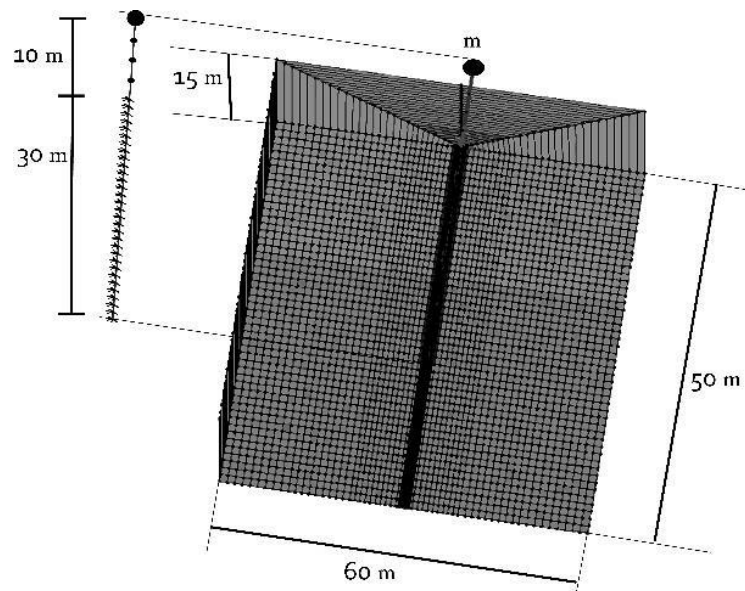
Figure 12. Mesh size of model
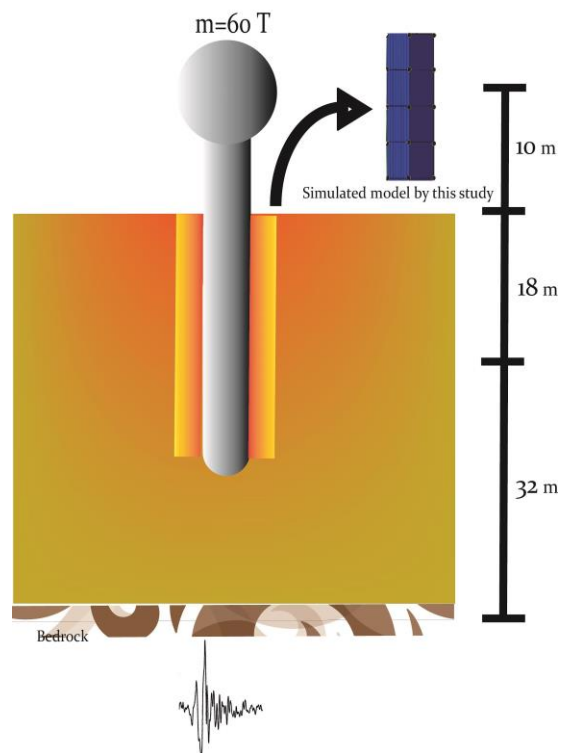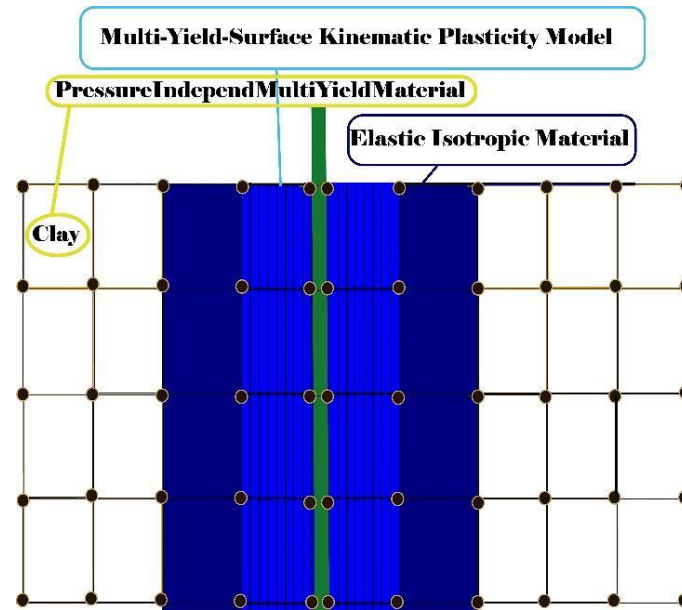

Figure 13. Simulated model

Figure 14. Modelling of soil pile interaction in Opensees

2.3. Properties of Soil

The crust of the earth consists of different soil types and soil is made naturally or chemically by weathering of rocks [23]. The inhomogeneous structure of soil makes the prediction of mechanical behavior is difficult. Clay is a common type of soil and has less strength. Clay that has been exposed to very high loads achieves a dense structure and becomes less compressible. When excavating in a clay layer, deformations occur. Due to this problem, there is a challenge to construct structures on a ground with deep layers of clay. In this study, two types of clay are used. Table 3 lists the properties of the soils considered in the pressure-in depend-multi-yield material of clays behavior. The soil profiles are uniform and the depth is 50 m (Figure 13). For both models, the same type of soil is used.

Table 3. Soil Properties

| Properties	Soft Clay	Stiff Clay
Mass Density (t/m^3)	1.6	1.8
Shear modulus (KPa)	49730.7	200000
Bulk modulus (KPa)	107749.9	433333.3
Poisson's Ratio	0.3	0.3
Cohesion (KPa)	26	100
Permeability co. eff (m/s)	10-9	10-7
Friction angle (deg.)	0	0
Peak Shear Strain	0.03	0.03
Number of Yield Surfaces	20	20

2.4. Input Ground Motion

Directivity effects and maximum acceleration are the basic parametric data used for choosing the time history of ground motion in Near Field and Far Field earthquakes. For this purpose, two records (with and without directivity effects (Table 4)) of strong motions of New Zealand were selected and Near Field, records were scaled to a peak acceleration value of 0.8 g. In addition, the peak of Far Field ground acceleration (PGA) was converted into 0.3g. Then, the deconvolution analysis was conducted with Opensees. Figure 15. shows the scaled version of these two free-field historic earthquake records utilized in this study. List of the earthquakes is included (Table 4). The response spectrum is designated at the rock level and the bedrock motion propagates to the surface.

Table 4. Directivity effects of records

Station	Earthquake	Pulse-Like Record
Christchurch Cathedral College	Christchurch New Zealand	-
PRPS	Christchurch New Zealand	+

Two records are selected in which Near Field ground motion has been classified into 2 categories: first, the record has strong velocity pulse; second, the Peak Ground Acceleration (PGA) of the Near Field record is 0.8 g. Records are presented in Figure 15 and Figure 16.
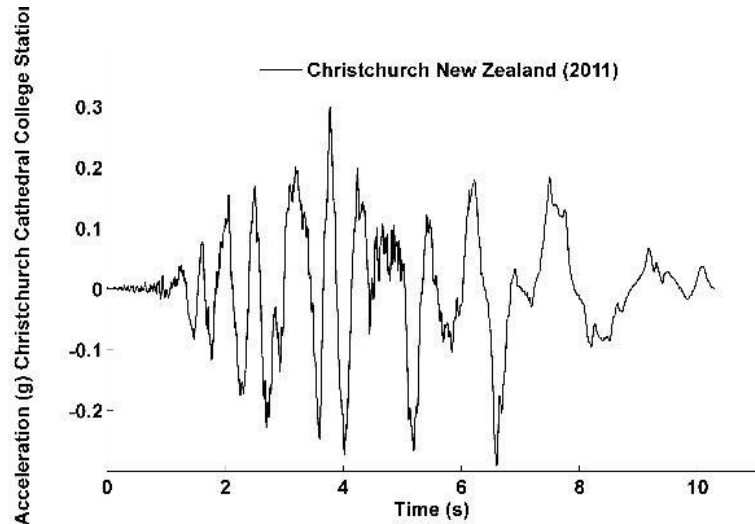
Figure 15. Far Field Accelerogram Scaled to Ag = 0.3 g
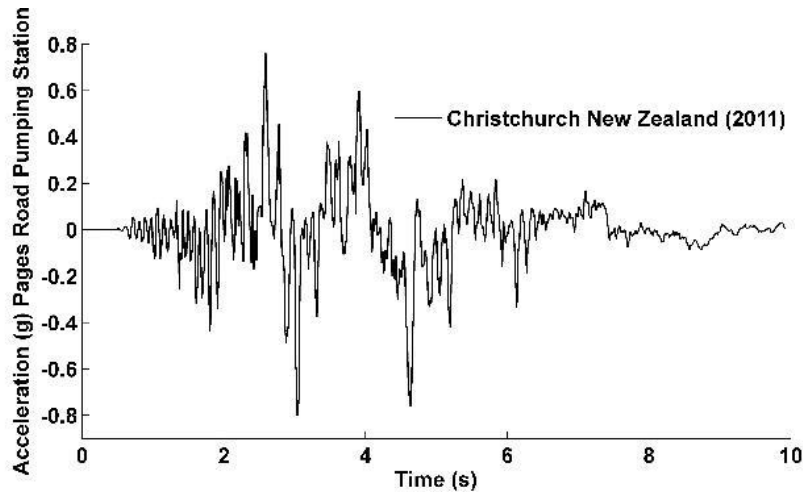
Figure 16. Near Field Accelerogram Scaled to Ag = 0.8 g

3. Results of Numerical Analyses and Comparison

The acceleration time histories of the deck level results of the numerical analyses are shown in Figure 17. and Figure 18 . Important distinctions between the Near Field and Far Field acceleration responses of the deck level of the structure are maximum acceleration response and period lengthening. Moreover, by comparing soil influence on the Near Field and Far Field, obviously, the seismic wave effects of Far Field earthquake are changed more than those 4 Near Field one with the softness of soils.
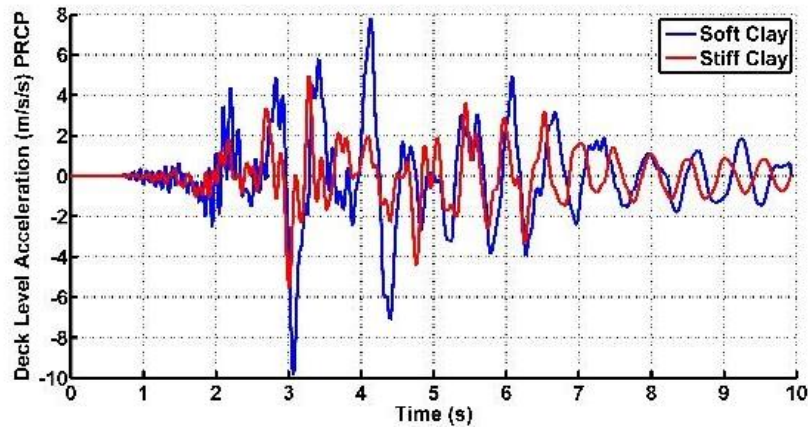
Figure 17. Comparison of acceleration response between soft clay and stiff clay (Near Field)
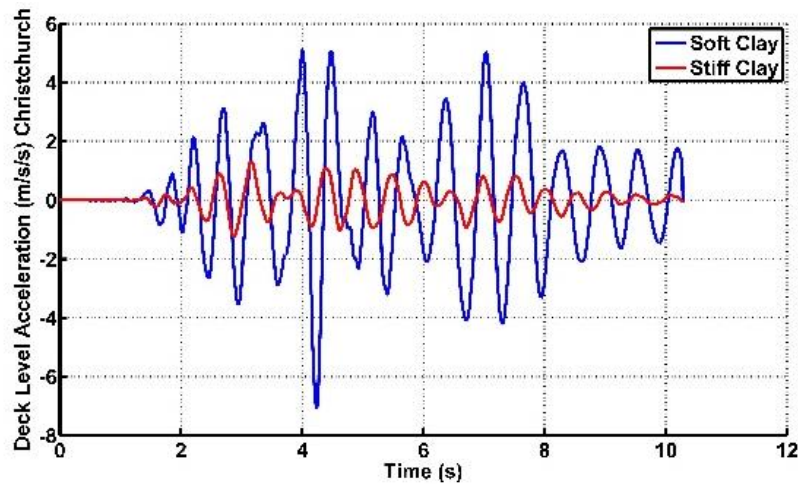

Figure 18. Comparison of acceleration response between soft clay and stiff clay (Far Field)

Figure 19 to 22. illustrate the various response of the displacement time history under the PRPS record (Far Field) and Cathedral College S record (Near Field) with 0.3 g and 0.8 g peak ground acceleration. The maximum displacement is found to be 6.3 mm at the top of the column-pile (Near Field- soft clay). Due to the soil effects, peak displacement response of the structure on stiff clay occurs earlier than that of soft clay (for Christchurch (Far Field) is found to occur at around 4.2 s, while that of stiff one is around 2.4 s and for PRP (Near Field) is found to happen at around 3.2 s for soft clay, although that is around 3.0 s for stiff one).
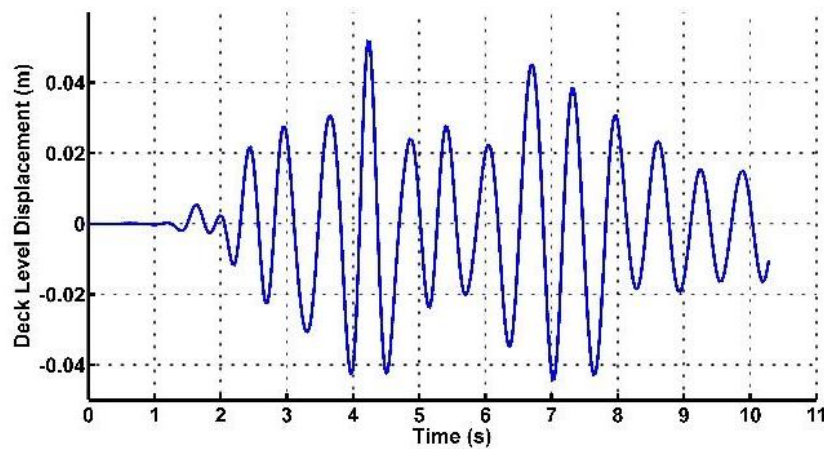

Figure 19. Displacement time history of the deck level for Far Field (Soft Clay)
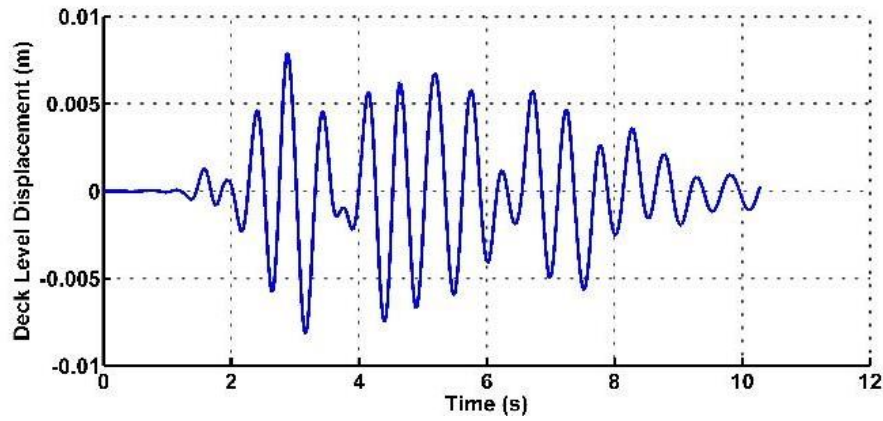
Figure 20. Displacement time history of the deck level for Far Field (Stiff Clay)
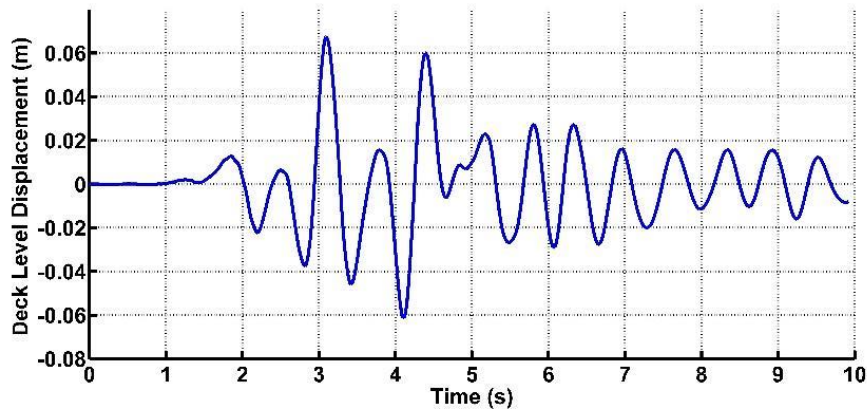

Figure 21. Displacement time history of the deck level for Near Field (Soft Clay)
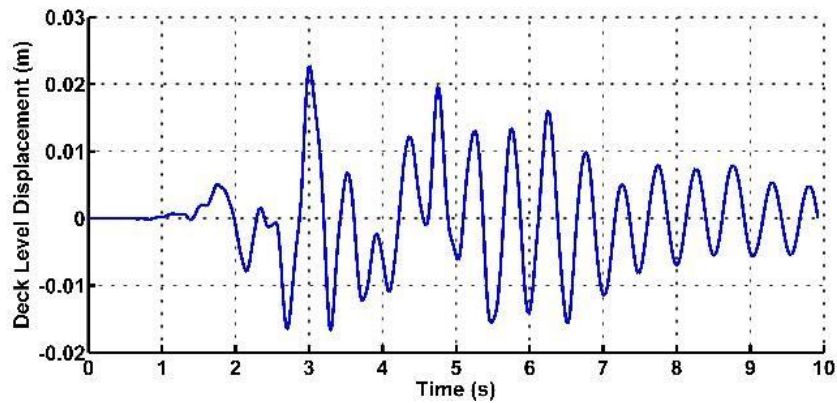

Figure 22. Displacement time history of the deck level for Near Field (Stiff Clay)

The maximum horizontal displacements along elevation of column-pile are displayed in Figure 23. As shown in the figure, the displacement of soft clay behavior analyses results are more than stiff ones. Results show lateral structure movement on not only soil, lateral displacement at the top of the structure and nonlinear components of soil response depend on soil properties but also earthquake record characteristics. Maximum lateral displacement at the top level of structure embedded in soft soil is more than the one in soil.
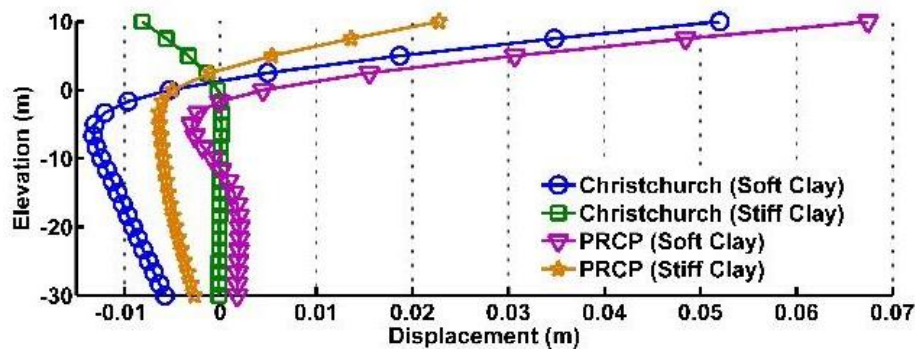
Figure 23. Results of maximum horizontal displacement of column-pile

4. Summary and Conclusions

This paper compares results from Near Field and Far Field earthquakes in three types of clay soil profiles that are one layer of soft clay, a stiff one layer and two soil layers, soft clay on the top of stiff clay. Elements of column-pile and soils are linked with materials instead of springs. The following salient conclusions were drawn based on the comparison of analytical results:

- Double layer of clay (soft clay above stiff clay) significantly increases the acceleration and displacement time history of the deck level column-pile.

- The inertial interaction effects of column-pile deck level in two-layer clay are more effective than kinematic interaction effects and it increases the deck level displacement. However, structure embedded in a layer of soil is more influenced by the kinematic interaction effects.

- Earthquake excitation, different soil types, and soil stratification use is in direct relation to change the column-pile and soil behavior.

- Proposed model with the nonlinear and linear material is validated by the p-y spring models.

- Soft clay soil increases the response of acceleration time history of structures in Far Field.

- Increasing and changing the Far Field horizontal accelerations due to softness of soils are more than Near Field horizontal accelerations. Consequently, site effects and soil tests of Far Field region are more imperative than Near Field one.

5. Acknowledgements

6. References

[1] S. Grimaz and P. Malisan, "Near field domain effects and their consideration in the international and Italian seismic codes," Bollettino di Geofisica Teorica ed Applicata 55(4), pp. 717-738, 2014.

[2] B. A. Bolt and N. A. Abrahamson, 59 –Estimation of strong seismic ground motions, In Lee W, Kanamori H, Jennings CP, Kisslinger C, editors.: International Handbook of Earthquake and Engineering Seismology-Part B. Academic Press [Chapter VII], 2003.

[3] P. G. Somervile, "Magnitude scaling of the near fault rupture directivity pulse," Physics of the Earth and Planetary Interiors 137, pp. 201-212, 2003.

[4] M. K. Kim, J. S. Lee and M. K. Kim, "Vertical Vibration Analysis of Soil-pile Interaction Systems Considering the Soil-pile Interface Behavior," KSCE Journal of Civil Engineering 8(2), pp. 221-226, 2004.

[5] [NFE05] EN 1997 -1. EUROCODE 7, "geotechnical design-part 1: general rules. 145p," 2005.

[6] G. Gazetas, V. Droses and N. Gerolymos, "Seismic response of single-column bent on pile: Evidence of beneficial role of pile and soil inelasticity," Bulletin of Earthquake Engineering, Vol. 7, No. 2, pp. 547-573, 2009.

[7] H. B. Mason, "Seismic Performance Assessment in Dense Urban Environments. (Doctoral dissertation)," University of California at Berkeley, Berkeley, CA, 2011.

[8] P. G. Somerville, "Characterizing Near Fault Ground Motion For The Design And Evaluation Of Bridges," in Third National Seismic Conference & Workshop on Bridges & Highways, Portland, Oregon, 2002.

[9] C. A. Felippa, "A Family of Early-time Approximations for Fluid-Structure Interaction," Journal of Applied Mechanics, 47, pp. 703-708, 1980.

[10] J. Lysmer and R. L. Kuhlemeyer, "Finite Dynamic Model for Infinite Media"," Journal of the Engineering Mechanics Division, Proc ASCE, Vol. 95, no. EM4, pp. 859-877, 1969.

[11] J. P. Wolf, Dynamic Soil-Structure-Interaction, Prentice-Hall, Englewood: Cliffs, New Jersey, 1985.

[12] Y. M. A. HASHASH and D. PARK, "SOIL DAMPING FORMULATION IN NONLINEAR TIME DOMAIN SITE RESPONSE ANALYSIS," Journal of Earthquake Engineering 8(2), pp. 249-274, 2004.

[13] T. Haukaas and A. Der Kiureghian, "Finite element reliability and sensitivity methods for performance-based Earthquake Engineering," PEER (Pacific Earthquake Engineering Research Center), University of California, Berkeley, April 2004.

[14] A. E. Kampitsis, E. J. Sapountzakis, N. Giannakos and N. A. Georolymos, "Seismic soil–pile–structure kinematic and inertial interaction—A new beam approach," Soil Dynamics and Earthquake Engineering 55, pp. 211-224, 2013.

[15] A. Elgamal, Z. Yang and E. Parra, "Computational modeling of cyclic mobility and post-liquefaction site response," Soil Dynamics and Earthquake Engineering 22(4), pp. 259-271, 2002.

[16] J. H. Prevost, "Anistropic Undrained Stress-Strain Behavior of Clays," Journal of the Geotechnical Engineering Division, ASCE, 104(GT8), pp. 1075-1090, 1978.

[17] J. P. Stewart, A. O. Kwok, Y. M. A. Hashash, N. Matasovic, R. Pyke, Z. Wang and Z. Yang, "Benchmarking of Nonlinear Geotechnical Ground Response Analysis Procedures," Report No. PEER-08/04, Berkeley, California, 2008.

[18] Q. Gu, J. P. Conte, A. Elgamal, and Z. Yang, "Finite-element response sensitivity analysis of multi-yield-surface J2 plasticity model by direct differentiation method," Computer methods in applied mechanics and engineering 198(30-32), pp. 2272-2285, 2008.

[19] Q. Gu, J. P. Conte, and A. Elgamal, "Consistent tangent moduli for multi for multi-yield-surface J2 plasticity model," Computational Mechanics 48(1), pp. 97-120, 2011.

[20] S. Wang, B. L. Kutter, J. M. Chacko, D. W. Wilson, R. W. Boulangar and A. Abghari, "Nonlinear seismic soil-pile-superstructure interaction," Earthquake Spectra Vol.14, Issue 2, pp. 377-396, 1998.

[21] A. E. Kampitsis, E. J. Sapountzakis, S. K. Giannakos and N. A. Gerolymos, "SEISMIC SOIL-PILE INTERACTION — INFLUENCE OF SOIL INELASTICITY," in 4th ECCOMAS Thematic Conference on Computational Methods in Structural Dynamics and Earthquake Engineering, Kos Island, Greece, 12-14 June 2013.

[22] S. Mazzoni, F. McKenna and G. Fenves, "Open System for Earthquake Engineering Simulation User Manual," Pacific Earthquake Engineering Research Center, Berkeley University (http://opensees.berkeley.edu/), California, 2006.

[23] S. Helwany, Applied Soil Mechanics with Abaqus Applications, Hoboken, New Jersey, ISA: John Wiley and Sons, ISBN:9780471791072, 2007.